Binary Droplet Coalescence – Influence of Ions and Mass Transfer

Jens S. HEINE[1,*], Felix GEBAUER[1], Christian WECKER[2], Eugeny Y. KENIG[2] and Hans-Jörg BART[1]

[1]*Chair of Separation Science and Technology, University of Kaiserslautern, Kaiserslautern, 67663, Germany;* [2]*Chair of Fluid Process Engineering, Paderborn University, Paderborn, 33098, Germany*

The behavior of coalescence in liquid/liquid systems is determined by multiple factors, including the concentration and type of any continuous phase ions present. Their influence on the film drainage time was captured with a high speed imaging system. Higher coalescence probabilities were found to correlate with a simple drainage model. Another focus was the mass transfer during droplet formation. Here in situ analytics in the system toluene/acetonitrile/water was applied for the mass transfer direction from the dispersed to the continuous phase. Marangoni effects during droplet formation are the reason that more than 75 % of the mass transfer occurs in the first 5 seconds, which agrees with the literature data reporting up to 80 %. Therefore, initial droplet formation (< 5 seconds) was also investigated by in silico experiments. The corresponding CFD studies were based on volume capturing methods.

1. Introduction

In chemical, biochemical and petrochemical processes, mass transfer in liquid/liquid extraction is of vital importance. The process efficiency and product quality in technical processes are substantially influenced by the interfacial area, which depends on the competitive dynamic phenomena of droplet breakage and coalescence. Despite comprehensive scientific research efforts, the influencing factors (e.g. pH value, salts, mass transfer), especially for coalescence, are not fully understood, and thus predictive modelling is not yet possible [2, 3].

The influence of the drainage on coalescence outcomes has been described in literature by various models. The most widely used approach of Coulaloglou and Tavlarides [4] assumes the coalescence probability as a ratio of drainage to contact time. A simplified relation [4] was used to describe the dependence of coalescence probability λ on the ratio of drainage $t_{drainage}$ to contact time $t_{contact}$, and the model of Coulaloglou and Tavlarides [4] is expanded via an additional exponent χ:

$$\lambda_{C\&T} = \exp\left(-\frac{t_{drainage}}{t_{contact}}\right)^{\chi} \quad (1)$$

The influence of ionic species on coalescence is reported, but scarcely systemically investigated [5]. A classification according to Hofmeister [6] is based on the precipitation effect, which distinguishes between cosmotropic and chaotropic ions. In the following sequence, cosmotropic ions are placed left and chaotropic right:

$$F^- \approx SO_4^{2-} < HPO_4^{2-} < CH_3COO^- < Cl^- < NO_3^- < Br^- < Clo_3^- < I^- < ClO_4^- < SCN^- < Cl_3CCOO^- \quad (2)$$

Structure forming ions (cosmotropic) intensify hydropobic effects, which are responsible for the separation of oil/water mixtures.

Regarding the mass transfer, a local (tangential) shear stress condition (e.g. a concentration dependent interfacial tension gradient) reflects a strong coupling between the velocity and the concentration fields. Marangoni instabilities (interfacial flow) are observed [7] when interfacial tension gradients are inducted by gradients in the solute concentration. In such cases, up to 80 % of the mass transfer occurs already during droplet formation [8].

The concentration profile in a droplet can be described as [9, 10]:

$$Fo_{tu} \leq 0.15: \qquad \frac{y(t)-y_I}{y_0-y_I} = 1-6\cdot\sqrt{\frac{Fo_{tu}}{\pi}}+3\cdot Fo_{tu} \tag{3}$$

with $Fo_{tu} = \frac{4\cdot D_{tu}\cdot t}{d^2}$ and $D_{tu} = T\cdot D$

where *Fo* stays for Fourier number, *y* for mass fraction of the transfer component, *D* for diffusion coefficient, *t* for time, *d* for droplet diameter, *T* for intensification factor.

When applying Equation 3 to describe experimental data, *T* is regarded as an adjustable parameter, since the turbulent eruptions have not yet been quantified. Model improvements require a high spatial and temporal resolution of the local phenomena, which is difficult to achieve experimentally. The possibility to overcome these limitations is given by computational fluid dynamics (CFD) simulations. In our study, the open-source CFD package OpenFOAM® was used. A standard volume-of-fluid (VOF) solver was extended with the mass transfer model of Haroun [11], adjusted boundary conditions and some improvements for the curvature approximation to reduce spurious currents.

2. Materials and methods

2.1 Experimental setup

The influence of ionic species and pH on coalescence was investigated with sodium chloride (Merck 1.06404), sodium nitrate (VWR chemicals 27955.295), sodium perchlorate (Merck 1.06564), sodium thiocyanate (Sigma-Aldrich S7757-250G) and sodium sulfate (VWR chemicals 28114.296). Sodium hydroxide (Merck 1.09956) was used to adjust the pH value. Water and toluene were mutually saturated in order to avoid additional mass transfer. Acetonitrile (ACN) as solute and toluene as solvent were of a purity > 99.8 % (CHROMANORM®). Water (conductivity of < 0.5 $\mu S\cdot cm^{-1}$) was purified by reserved osmosis (Hydrotec, Hydromos UO 50 W) and ion exchange (Hydrotex, Hydromos VE 17).

Constant and reproductive test conditions for the droplet generation (precision syringe pump, PSD/3-Mini module, from Hamilton®), detachment and interaction were ensured with a coalescence cell after Kamp and Kraume [12]. A high speed camera (Photron Fastcam APX RS) recorded videos with a resolution of 256x256 pixels and a frame rate of 30000 fps. The size of the rising droplet d_b (at constant rising height of 0.5 mm to the hanging droplet d_u) was systematically varied, in order to adjust the equivalent droplet diameter d_{eq}:

$$d_{eq}=2\cdot\frac{d_u \cdot d_b}{d_u + d_b} \quad (4)$$

The mass transfer and the effect of Marangoni convection during droplet formation was identified by measuring the interfacial tension as a function of time, as well as by measuring the concentration inside the droplet by non-invasive confocal Raman spectroscopy.

Measurement methods:

- A newly designed test cell for single droplet mass transfer [13] was made of stainless steel and PTFE, with a capillary height of 2 mm and the inner dimensions of 33 mm*23 mm*33 mm (*L*W*D*). The droplet is formed on a capillary, which has an inner diameter of 0.8 mm and an outer diameter of 1 mm. A precision syringe pump (PSD/3-Mini module) from Hamilton® was used to generate well-defined droplets with a volume rate of $\dot{V}$=12.5 µL·s^{-1}. The solute concentration inside the droplet was measured via a confocal Raman spectrometer HR800 from Horiba (532 nm laser from Quantum, type torus 532, software LabSpec6).
- The pendant drop method was used to determine the interfacial tension (OCA 15; Dataphysics) with a syringe in the surrounding phase in which the contact angles of a single droplet were measured. The curved syringe is used for the investigation of the pendant drops with an inner diameter of 0.69 mm and an outer diameter of 1.07 mm and a Hellma® glass-measuring cell [13] with the inner dimensions of 50 mm*50 mm*10 mm (*L*W*D*). The respective droplets were formed at a volumetric rate of $\dot{V}$= 2 µL·s^{-1}.

3. Results and discussion

3.1 Experimental

3.1.1 Ion species and strength

Experimentally determined coalescence probabilities and times are compared with the simplified correlation (s. Equation 1) in Figure 1. The coalescence probability was observed to decrease with increasing coalescence times for each ion species investigated, when adjusting the exponent χ = 1.6. An average contact time of 25 ms was used for the calculations of the theoretical coalescence probability. This assumption was chosen in accordance with the calculations of Villwock et al. [14].

Experimental outliers can be attributed to the high sensitivity of the coalescence process to marginal changes in the test system, which may

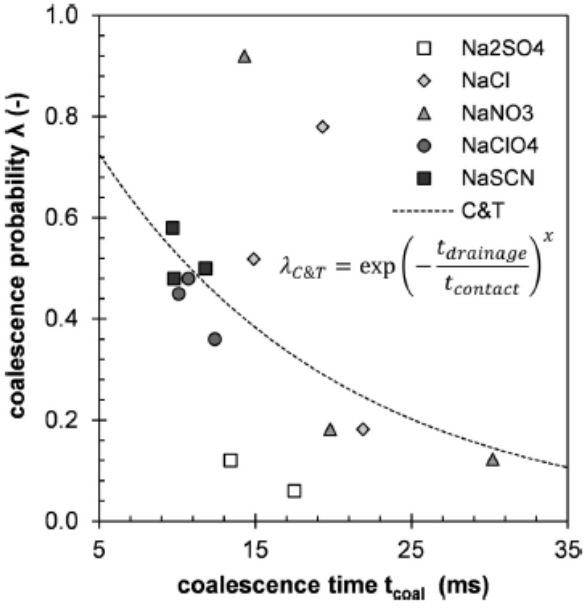

Figure 1. Effect of ionic species the coalescence time t_{coal}, for all d_{eq} [1]

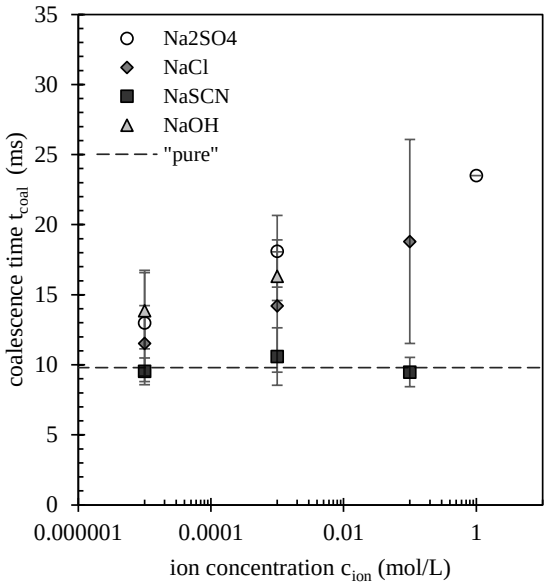

Figure 2. Coalescence probability vs. coalescence time for different ion species ($d_{eq} = 2.5\ mm$) [1]

Along with the influence of the ion species, the concentration is also of relevance (s. Figure 2). Increasing the concentration of chaotropic ion species (e.g. NaSCN) had a negligible effect on the coalescence time. In contrast, the coalescence time increased with the addition of cosmotropic anions (e.g. Na_2SO_4).

A description of the ion influence is required that is independent of the equivalent droplet diameter is possible, through the extension of the model of Prince et al. [15] with the newly developed Equation 5. Here the coalescence time is mapped over the entire range of salt concentrations using c_1 and c_2 to correlate different ion species:

not lead to a measureable change in physical properties (e.g. interfacial tension).

According to the aforementioned Hofmeister anion species classification (s. Equation 2), cosmotropic, structure-forming, anions were observed to slow down the drainage rate. For example, the addition of sodium sulfate increased the coalescence time as compared to the "pure" system (s. Figure 2). Chaotropic, structure-destroying, anions, such as SCN^-, have a significantly lower impact on the coalescence time.

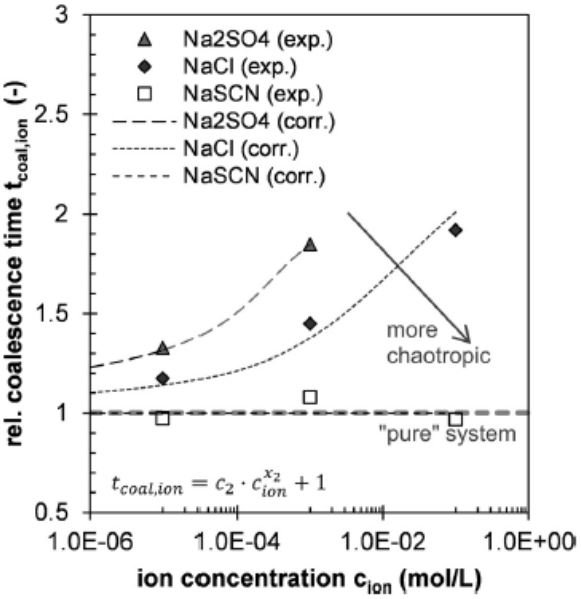

Figure 3. Effect of NaCl concentration on the coalescence time compared to correlation, Equation 5 [1]

$$t_{coal,P\&B^*,NaCl} = \left[\frac{\left(\frac{d_{eq}}{2}\right)^3 \cdot \rho_c}{16 \cdot \sigma}\right]^{\frac{1}{2}} \cdot \ln\left(\frac{h_0}{h_{crit}}\right) \cdot (c_1 \cdot c_{ion}^{c_2} + 1) \quad (5)$$

where t_{coal} is coalescence time, d_{eq} is equivalent droplet diameter, ρ is density, σ is interfacial tension, h_0 is film thickness at the point of contact, h_{crit} is critical film thickness, c_{ion} is ion concentration and c_1, c_2 are constants.

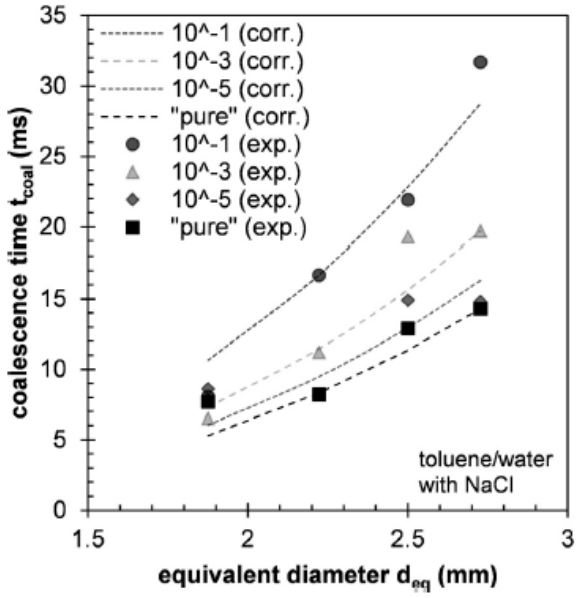

Figure 4. Effect of increasing NaCl concentration on the coalescence time according to Equation 5 [1]

3.1.2 Mass transfer measurement with Raman spectroscopy

The confocal Raman spectroscopy measurement in a droplet with an initial solute concentration of $c_{ACN} = 10$ w.-% and a volume of 4.2 µL shows a decrease of the solute concentration over time (s. Figure 5). It can be seen that the concentration decreases very fast, so that 90 % of the mass transfer occurs during the first 5 seconds. This fast decrease in concentration can be described with Equation 3 for turbulent mass transfer ($T = 25$) and follows the measurement results in the first 10 seconds very well.

The change in the coalescence time with the addition of e.g. sodium chloride ($c_1 = 1.652$, $c_1 = 0.214$) shown in Figure 3. Equation 5 enables a description of the coalescence time for changing ion concentrations of sodium chloride without adjustment (s. Figure 4).

However, Equation 5 is only valid below ionic concentrations of 10^{-1} mol/L and in the range of equivalent droplet diameters of 1.87 mm < d_{eq} < 2.73 mm for the EFCE standard test system toluene/water.

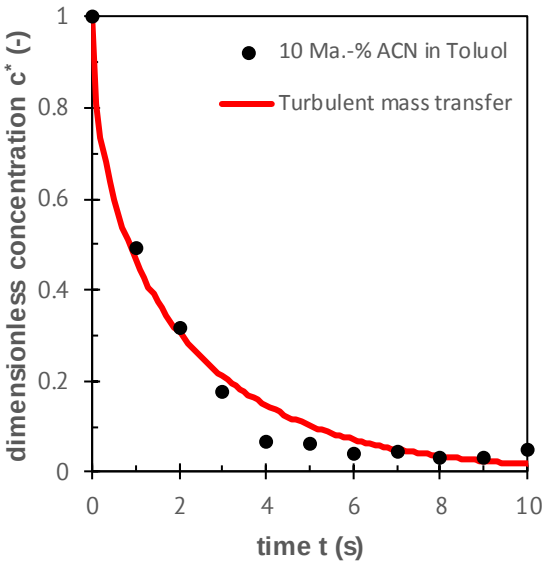

Figure 5. Transient development of the solute concentration on a droplet ($V = 4.2$ µL) with an initial solute concentration of $c_{ACN} = 10$ w.-% and a flow rate $\dot{V} = 12.5$ µL·s^{-1}

3.1.3 Mass transfer measurement via interfacial tension

Interfacial tension measurements need a higher droplet volume compared to Raman spectroscopy, and hence, droplet formation has to be slower, otherwise the droplet will be detached from the needle. However, after about 7.5 seconds the droplet has gained its final shape with a corresponding stable mass transfer behavior. The measurement with an initial solute concentration of $c_{ACN} = 10$ w.-% and a volume of 15 µL shows that the first measurement points (s. Figure 6) lead to either decreased or increased interfacial tension. Therefore, the dimensionless concentration is either too high or too low in the first seconds. Nevertheless, in the first 5 seconds more than 75 % of the mass transfer occurred. However, the correlation (s. Equation 3) with $T = 8$ fits the measurement results after 20 seconds very well.

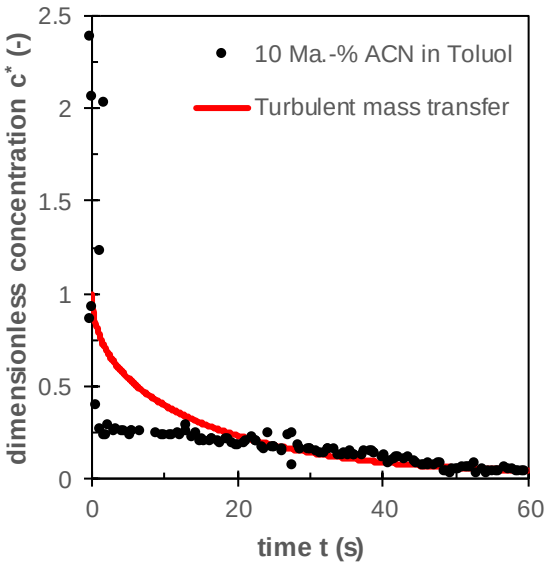

Figure 6. Interfacial tension measurements of the solute concentration on a droplet (V = 15 µL) with an initial solute concentration of c_{ACN} = 10 w.-% and a flow rate $\dot{V}$ = 2 µL·s^{-1}

As could be seen, both methods were unable to monitor mass transfer in the first seconds of droplet formation. Raman spectroscopy has its focus on measurement inside the droplet and interfacial tension on measurement the surface of the droplet; thus deviations between these measurements exists. Thereto, in silico experiments with small time steps are necessary. Here, CFD methods can be applied to reveal temporal and spatial details.

3.2 Numerical simulations

Coalescence

In respect to droplet coalescence of e.g. two differently sized droplets (pendant with 2.2 mm and top with 3 mm), simulation using a modified VOF code, (s. Figure 7, top) were compared with the experimental data (s. Figure 7, bottom) [16]. The simulated sequence of the simulation is given by a 2D plot as a cut through the center of the domain. Before the droplets enter into actual contact, the increasing pressure in the film between them leads to an elliptical droplet deformation. After 19.1 ms, similar droplet shapes and film rupture can be observed both in the simulations and in the experiments.

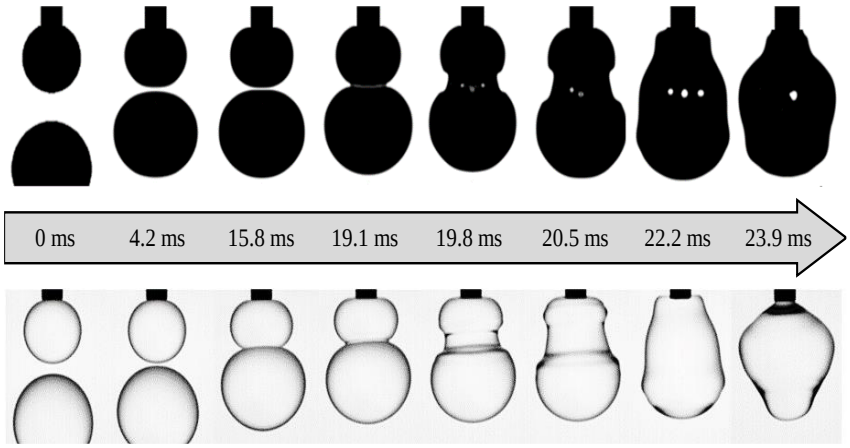

Figure 7. Coalescence toluene/water; CFD (top); exp. (bottom) [16].

Mass transfer

At first, the extended solver has to be validated to ensure that the results are confident. Therefore, a VOF simulation of a single falling droplet (d = 2.5 mm) in a quiescent liquid was performed. The concentration decrease over the time was compared with a validated level-set code from Engberg [17] (s. Figure 8). The standard test system cyclohexane/water/acetic acid in which water represents the continuous phase and acetic acid the transition component was studied in a two dimensional mode. As can be seen, the mass transfer model yields restorable results, but it seems to be important to reduce the spurious currents. For simulation of droplet formations, further studied will follow.

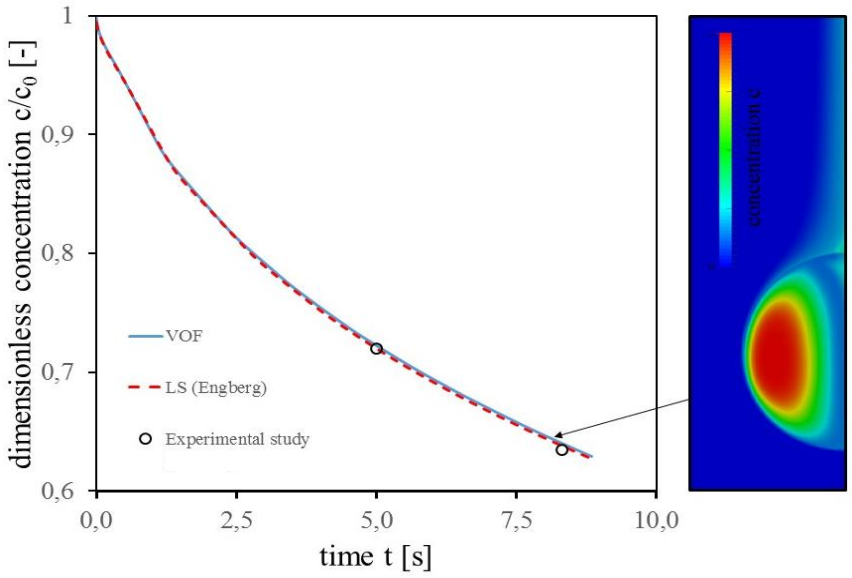

Figure 8. Dimensionless average concentration in the droplet over time (left); concentration field after eight seconds (right)

4. Conclusions

Systematic experiments to investigate the dynamic coalescence of two organic droplets were carried out, with the focus on the variation of the ionic strength and ion species. To meet the high requirements of reproducibility and purity, a standardized and validated experimental setup was used. Characteristic coalescence times were measured using a high speed camera with high temporal and spatial resolution. Cosmotropic anions lead to a significant increase in the coalescence time, the addition of chaotropic anions did not change the coalescence time. Based on the present experimental results, a correlation was developed to predict the dependency of the coalescence time on both the equivalent droplet diameter and ion concentration.

The influence of the Marangoni convection on the mass transfer during droplet formation was evaluated with the chemical system toluene/acetonitrile/water applying two different analytical methods. In the first method, the measurement of the solute concentration inside the droplet at a defined area was performed by confocal Raman spectroscopy. The measurement of the mass transfer inside a single droplet (V = 4.2 µL) showed that, with a droplet formation time of 0.34 seconds and an initial solute concentration of c_{ACN} = 10 w.-%, about 90 % of the mass transfer occurred during the first 5 seconds. However, this is not consistent with the interfacial tension measurements at the droplet surface. Under similar concentration conditions with a droplet formation time of 7.5 seconds (V = 15 µL), a value of 75 % of the initial surface concentration was reached in the first 5 seconds.

This discrepancy between the interfacial tension measurements and the confocal Raman spectroscopy can be explained by the difference in droplet formation time, droplet volume and the measurement inside and on the surface of the droplet. On the other hand, similar trends can be obtained with both measurement methods, which means that a large part of the mass transfer after the droplet formation is

completed in the first seconds. For these first seconds, in silico experiments offer the possibility to enable a more detailed analysis.

The numerical investigation of single droplet interactions opens up several possibilities for the model development. On the one hand, local spatial and time resolved information about the hydrodynamics and the film drainage will allow a better understanding of the coalescence behavior. On the other hand, detailed numerical VOF based simulations will help to determine surface and bulk droplet concentrations with high temporal resolution thus allowing a deep insight into mass transfer and droplet formation phenomena.

Acknowledgement

The authors gratefully acknowledge the financial support of the German Research Foundation (DFG) for this work (BA 1569/73-1, KE 837/28-1).

References

[1] F. Gebauer, J. Villwock, M. Kraume, H.-J. Bart, *Chem. Eng. Res. Des.*, **115**, 282 – 291 (2016).
[2] R. T. Eiswirth, Binary coalescence of free rising droplets, *Dissertation*, TU Kaiserslautern (2014).
[3] M. Henschke, *Chem. Eng. J.*, **85**, 369 – 378 (2002).
[4] C. A. Coulaloglou, L. L. Tavlarides, *Chem. Eng. Sci.*, **32**, 1289 – 1297 (1977).
[5] A. Pfennig, A. Schwerin, *Ind. Eng. Chem. Res.*, **37**, 3180 – 3188 (1998).
[6] F. Hofmeister, *Archiv f. experiment. Pathol. u. Pharmakol*, **25**, 1 – 30 (1888).
[7] M. Wegener, A. R. Paschedag, *Int. J. Multiphase Flow*, **37**, 76 – 83 (2011).
[8] L. Steiner, G. Oezdemir, S. Hartland, *Ind. Eng. Chem. Res.*, **29**, 1313 – 1318 (1990).
[9] A. B. Newman, *Trans. AIChE ,***27**, 310 – 333 (1931).
[10] A. B. Newman, *Trans. AIChE ,***27**, 203 – 220 (1931).
[11] Y. Haroun, Etude du transfert de masse réactif Gaz-Liquide le long de plans corrugués par simulation numérique avec suivi d'interface, *Dissertation*, Université de Toulouse (2008).
[12] J. Kamp, M. Kraume, *Chemical Engineering Research and Design*, **92**, 635 – 643 (2014).
[13] J. S. Heine, C. Wecker, E. Y. Kenig, H.-J. Bart, *Stofftransport bei der binären Tropfenkoaleszenz*, Jahrestreffen der Fachgruppe Extraktion, Köln (2017).
[14] J. Villwock, F. Gebauer, J. Kamp, H.-J. Bart, M. Kraume, *Chem. Eng. Technol.*, **37**, 1103 – 1111 (2014).
[15] M. J. Prince, H. W. Blanch, *AIChE J.*, **36**, 1485 – 1499 (1990).
[16] F. Gebauer, M. W. Hlawitschka, H.-J. Bart, *Chin. J. Chem. Eng.*, **24**, 249 – 252 (2016).
[17] R. F. Engberg, Einzeltropfen in Flüssig-flüssig-Systemen: Numerische Untersuchungen zu Fluiddynamik, Stofftransport und Marangonikonvektion, *Dissertation*, Universität Paderborn (2016).